ISBN: 978-3-95450-214-1 ISSN: 2673-5490 doi:10.18429/JACoW-IPAC2021-TUPAB041

DETECTOR SOLENOID COMPENSATION FOR THE ELECTRON-ION COLLIDER*

B. R. Gamage†, T. Michalski, V. S. Morozov, R. Rajput-Ghoshal, A. Seryi, W. Wittmer, Y. Zhang
Jefferson Lab, Newport News, VA, USA
A. Kiselev, H. Lovelace III, B. Parker, S. Peggs, S. Tepikian, F. Willeke, H. Witte, Q. Wu
Brookhaven National Lab, Upton, NY, USA
E. Gianfelice-Wendt, Fermilab, Batavia, IL, USA

Abstract

The central detector in the present EIC design includes a 4 m long solenoid with an integrated strength of up to 12 Tm. The electron beam passes on axis through the solenoid, but the hadron beam has an angle of 25 mrad. Thus, the solenoid couples horizontal and vertical betatron motion in both electron and hadron storage rings, and causes a vertical closed orbit excursion in the hadron ring. The solenoid also couples the transverse and longitudinal motions of both beams, when crab cavities are also considered. In this paper we present schemes for closed orbit correction and coupling compensation at the IP, including crabbing.

INTRODUCTION

To integrate the detector solenoid into the detector regions, we must resolve the following issues: 1) Closed orbit distortion; 2) Transverse beam focusing; 3) Polarization effect; 4) Rotation of the crabbing planes; 5) Transverse coupling [1, 2]. These effects need to be studied and if needed, properly compensated, to maintain the high luminosity requirements as noted in the EIC design report [3].

CLOSED ORBIT CORRECTION

The hadron beam line goes through the detector solenoid at a 25 mrad angle. This causes horizontal displacements of both east and west fringe fields of the solenoid, which leads to the hadron beam experiencing a vertical kick. We choose an orbit correction scheme that minimizes the size and extent of the orbit excursion given the spacial constraints for corrector placement. Figure 1 shows the vertical (y) orbit excursion and the orbital angle in the IR. Horizontal (x) orbit excursion is significantly smaller compared to y. With the current placement of kickers [4], there is a ~0.75 mm maximum excursion in the final focusing quadrupoles which may lead to stronger multipole effects on the beam dynamics.

POLARIZATION EFFECT

The polarization direction of the electron beam is aligned with the detector solenoid axis, which causes no change of the polarization direction. However, it causes an additional spin rotation [5] φ_s shifting the spin tune ν_s by

$$\Delta\nu_s = \frac{\varphi_s}{2\pi} = \frac{(1+G)}{2\pi}\frac{B_{sol}L}{B\rho}, \qquad (1)$$

where $G \approx 1.160 \cdot 10^{-3}$ is the electron's anomalous gyromagnetic ratio, $B_{sol}L$ is the solenoid field integral, and $B\rho$ is the electron magnetic rigidity. The spin tune shift $\Delta\nu_s$ reaches a maximum of about 0.115 with the strongest 3 T field of the 4 m long solenoid at the lowest electron energy of 5 GeV. The spin tune shift may affect spin matching and polarization lifetime and must be accounted for in the analysis of the electron polarization dynamics.

The proton spin rotation by each of the IR elements including the pitched solenoid can be calculated analytically. Therefore, the net spin effect of all elements combined can also be in principle obtained analytically. However, it is more efficient to calculate the range of the spin rotation directions and angles numerically. To quantify the spin effect of the orbit perturbation compared to the perfectly aligned case, we represent the additional spin effect of the perturbation by an effective spin-rotating element placed at the IP. Table 1 lists the components of the spin rotation axis (n_x, n_y, n_z) and the rotation angle φ_s of this effective element assuming a 3 T solenoid for a few characteristic proton energies.

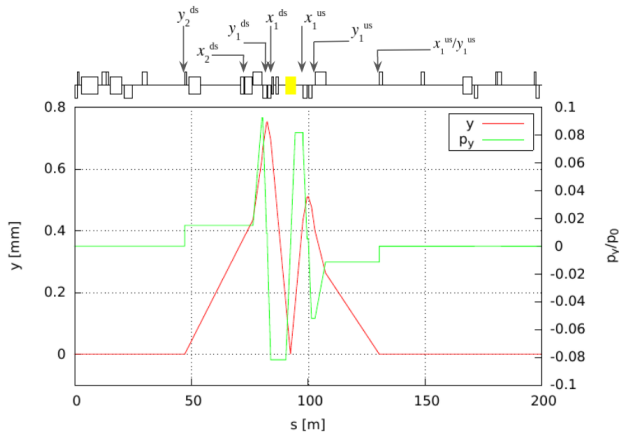

Figure 1: The vertical orbit offset and orbital angle are plotted against the distance s for 275 GeV protons. The arrows and labels shows the locations of the horizontal (x) and vertical (y) kickers in the IR. The yellow box indicates the placement of the detector solenoid.

* This material is based upon work supported by Jefferson Science Associates, LLC under Contract No. DE-AC05-06OR23177, Fermi Research Alliance, LLC under Contract No. DE-AC02-07CH11359, and Brookhaven Science Associates, LLC under Contract No. DE-SC0012704 with the U.S. Department of Energy.
† randika@jlab.org

ISBN: 978-3-95450-214-1 ISSN: 2673-5490 doi:10.18429/JACoW-IPAC2021-TUPAB041

Table 1: Spin Rotation Axis $(n_x,\ n_y,\ n_z)^*$ and Rotation Angle φ_s of the Effective Element at the IP Representing the Additional Spin Rotation in the Perturbed Orbit Case Compared to the Aligned Case for a few Characteristic Proton Energies

Energy (GeV)	n_x	n_y	n_z	$\varphi_s(2\pi)$
41	0.98	0.18	−0.076	0.038
100	0.97	0.23	−0.047	−0.035
200	0.93	−0.37	−0.029	0.021
275	0.88	−0.48	−0.025	−0.035

CORRECTION OF THE CRABBING PLANE ROTATION

Due to the small variation of the betatron phase advance from the detector solenoid to the crab cavities ($\simeq \pi/2$), it is not possible to completely compensate the coupling induced by the solenoid locally between the crab cavities using only skew quads. If coupling is not compensated between the crab cavities and IP, the solenoid rotates the transverse beam profile by $\theta_{sol}/2$. This effect is much greater on electrons due to their lower beam energies.

Since the aspect ratio of the beam spot size at IP is high, this may lead to a significant luminosity reduction. Moreover, as the bunch moves through the forward side of the solenoid, its crabbing plane continues to rotate doubling the tilt angle. The bunch arrives at the forward set of the crab cavities with its crabbing plane out of alignment with the plane of the compensating crabbing kick. Thus, the crabbing kick does not close and propagates around the ring.

A solution is to control the orientation of the kick plane at the crab cavities by adding a vertical component to the kick. If the horizontal and vertical crabbing kicks are adjusted so that the crabbing plane is tilted by an angle equal and opposite to the solenoid rotation angle the bunch arrives at the IP with its crabbing plane being horizontal as shown by the red points in Fig. 2. The tilt accumulated in the downstream part of the solenoid is compensated by adjusting the horizontal and vertical kicks and therefore the orientation of the kicking plane of the downstream crab cavities. The vertical kicks can be implemented by several additional crab cavities rotated by 90° with respect to the horizontal cavities. These additional units may also be necessary to account for coupling from sources other than the solenoid, misalignments and other imperfections.

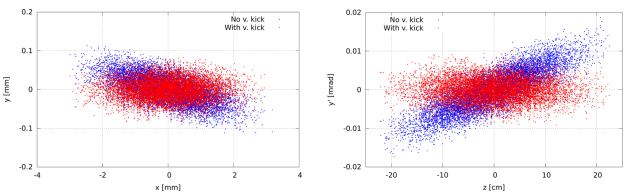

Figure 2: Tilt of the xy (left) and zy' (right) bunch phase space distributions at the IP due to the detector solenoid and its compensation by additional vertical crabbing kicks.

The required vertical crabbing voltage on each side of IP is given by,

$$V_y^{crab} = V_x^{crab} \sqrt{\frac{\beta_x^{crab}\beta_x^*}{\beta_y^{crab}\beta_y^*}}\,\frac{\theta_{sol}}{2}, \tag{2}$$

where V_x^{crab} is the horizontal crabbing voltage, β_x^{crab} and β_y^{crab} are the horizontal and vertical β functions, respectively, at the crab cavities, β_x^* and β_y^* are the horizontal and vertical β functions, respectively, at the IP, and θ_{sol} is the characteristic solenoid angle given by $B_{sol}L/2B\rho$. Assuming that $\beta_y^{crab} = \beta_x^{crab}$, the required electron and hadron V_y^{crab} are about 430 and 140 kV, respectively.

If the orbital motion is stable uncompensated crabbing kick results in a formation of an equilibrium 6D phase space ellipse at the IP with potentially correlated transverse and longitudinal degrees of freedom. To better understand which correlations can appear and their importance, we setup the model shown in Fig. 3 using linear matrices.

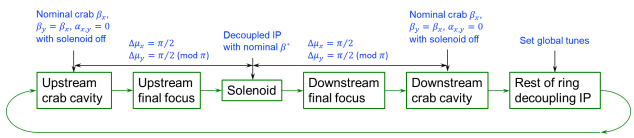

Figure 3: Schematic of the linear model used to study correlations generated by interaction of transversely coupled motion and crabbing dynamics.

The result of simultaneous implementation of the global coupling compensation and vertical crabbing kick correction is shown in Fig. 4. Figure 4 compares matched phase space distributions at the IP without and with a 3 T solenoid. There is no apparent effect of the solenoid on the beam distribution at the IP. Note that compensation using vertical crabbing kicks is less important for protons than electrons and can potentially be avoided. The importance and techniques for closing of the crabbing bump for electrons are currently being studied.

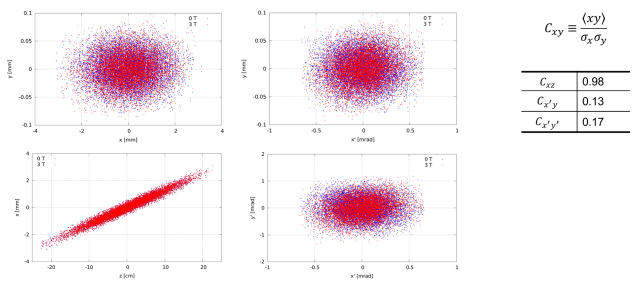

Figure 4: xy (top left), zx (bottom left), $x'y$ (top right) and $x'y'$ (bottom right) matched phase space distributions for the cases without a solenoid (blue) and with a 3 T solenoid (red) obtained using both global coupling and vertical crabbing kick corrections. The table on the right-hand side specifies the largest correlation coefficients.

ISBN: 978-3-95450-214-1 ISSN: 2673-5490 doi:10.18429/JACoW-IPAC2021-TUPAB041

COUPLING COMPENSATION

ESR

To preserve the polarization lifetime, it is essential to precisely compensate coupling of the electron beam as locally as possible. It must be done in a way that does not generate vertical dispersion outside of the coupled section. Ideally, to get orthogonal control of the off-diagonal matrix elements, the skew quadrupoles must be implemented with phase advance values $(\Delta\mu_x,\ \Delta\mu_y)$ between them as given by [1]

$$(\Delta\mu_x,\ \Delta\mu_y) : (\pi/2,\ 0), (\pi/2,\ \pi/2), (0,\ 0), \text{ and } (0,\ \pi/2)\ (\text{mod}\ \pi). \quad (3)$$

Since it was not possible to place the skew quads in these exact locations, we empirically identified locations in the existing lattice where the skew quads are as independent as possible. We added skew components to the existing straight quadrupoles in the matching sections between IP and electron spin rotators as shown in Fig. 5(top). We used 6 skew quads per side that have the strongest impact on coupling coefficients and also adjusted the strengths of 10 existing quads to keep the optics at the IP and the IR ends fixed at the design Twiss parameters.

The result of coupling compensation at 5 GeV where the solenoid induces the strongest coupling is shown in Fig. 5(top) using the Ripken parameterization of coupled β functions. β_{12} and β_{21} being zero along with their slopes indicates compensation of coupling. Correction of the vertical dispersion is shown in Fig. 5(bottom).

HSR

For the coupling compensation in the HSR, we rely on the existing knobs from RHIC. The main difference between RHIC vs HSR is that the EIC proton beam is flat with a horizontal to vertical emittance ratio of about 20 vs the round beams in RHIC. Still, the global decoupling scheme is adequate for hadrons with a slight change in regards to the number of knobs. For this, we identified six existing skew quad families of 4 skew quads per family. These families were used to correct the four off-diagonal transverse elements of the single-turn periodic orbital transfer matrix and the vertical dispersion D_y and its slope D'_y at the IP.

The resulting Ripken coupled β functions at 275 GeV are shown around the ring in Fig. 6. The maximum values of the coupling β functions β_{12} and β_{21} are less than 0.5 m compared the 2 km size of the uncoupled projections β_{11} and β_{22}. The maximum required gradient of the skew quads is about 1.3 T/m. The absolute values of the skew quad gradients are practically independent of the beam energy because of the constant solenoid field. The maximum and rms D_y are about 6.1 and 1.7 cm, respectively.

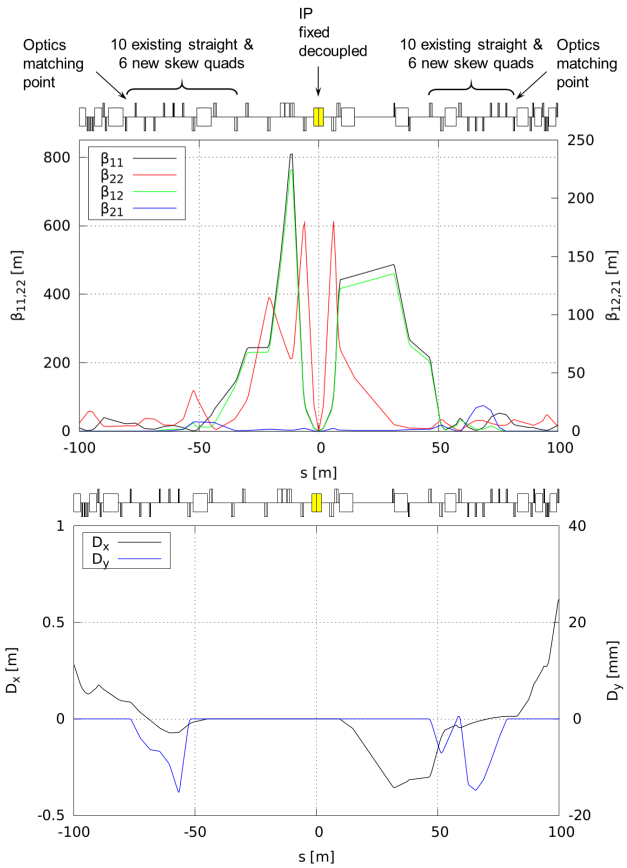

Figure 5: Ripken coupled β functions (top) and horizontal D_x and vertical D_y dispersions (bottom) in the electron interaction region after coupling compensation at 5 GeV.

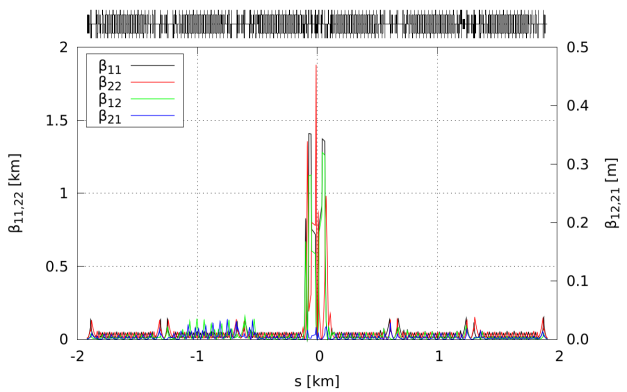

Figure 6: Ripken coupled β functions around the hadron collider ring at 275 GeV after coupling compensation and vertical dispersion correction.

SUMMARY

This paper provides a summary of the recent wok done towards the proper integration of the detector solenoid in the EIC. As the EIC design evolves, the compensation techniques discussed here can be applied with slight modifications (eg: kicker locations). Studies for compensation of the crabbing plane rotation are ongoing.

ISBN: 978-3-95450-214-1 ISSN: 2673-5490 doi:10.18429/JACoW-IPAC2021-TUPAB041

REFERENCES

[1] S. G. Peggs, "The projection approach to solenoid compensation", *Part. Accel.*, vol. 12, pp. 219-229, 1982. https://cds.cern.ch/record/136344/files/p219.pdf

[2] G. Wei *et al.* "Evaluation and compensation of detector solenoid effects in the JLEIC", in *Proc. 7th Int. Particle Accelerator Conf. (IPAC'16)*, Busan, Korea, May 2016, pp. 2454-2456. doi:10.18429/JACoW-IPAC2016-WEPMW015

[3] J. Beebe-Wang *et al.*, "Electron Ion Collider eRHIC Pre-Conceptual Design Report", BNL, NY, USA, Rep. BNL-211943-2019-FORE, 2019.

[4] J. S. Berg and H. Lovelace III, private communication.

[5] A. Kondratenko *et al.*, "Impact of the tilted detector solenoid on the ion polarization at JLEIC", *J. Phys.: Conf. Ser.*, vol. 938, p. 012021, 2017. doi:10.1088/1742-6596/938/1/012021